Chinese Chemical Letters 32 (2021) 543–547

Contents lists available at ScienceDirect

Chinese Chemical Letters

journal homepage: www.elsevier.com/locate/cclet

Communication

Ultrafast room-temperature reduction of graphene oxide by sodium borohydride, sodium molybdate and hydrochloric acid

Jun Hu, Gang Kong*, Yanbin Zhu, Chunshan Che

School of Materials Science and Engineering, South China University of Technology, Guangzhou 510641, China

ARTICLE INFO

Article history:
Received 16 December 2019
Received in revised form 19 January 2020
Accepted 17 March 2020
Available online 19 March 2020

Keywords:
Carbon materials
Reduced graphene oxide
Sodium borohydride
Sodium molybdate
Hydrochloric acid
Supercapacitors

ABSTRACT

Since graphene-based materials have shown great potential in many fields, it is important to explore ultrafast and high-efficient methods to synthesize reduced graphene oxide (rGO) using inexpensive reducing agents under mild conditions. Here, we reported a novel method for the ultrafast chemical reduction of graphene oxide (GO) at room temperature using sodium borohydride ($NaBH_4$), sodium molybdate (Na_2MoO_4) and hydrochloric acid (HCl). The reduction was carried out within 2 min. A series of characterization results revealed that the obtained reduced graphene oxide has higher reduction degree than that synthesized by $NaBH_4$ alone at high temperature. Moreover, rGO electrode based on the present reducing method exhibited a superior specific capacitance of 139.8 F/g at a current density of 1 A/g, indicating that it can be used as electrode materials for supercapacitors.

Graphene has attracted continually attention due to its unique structure and properties [1,2]. So far, two approaches are commonly used towards the production of graphene, the bottom-up approach starting with simple carbon molecules such as chemical vapor deposition [3] and epitaxial growth [4], or a top-down approach starting with graphite such as exfoliation [5] and chemical oxidation and reduction [6]. Among them, chemical oxidation and reduction is one of the most promising approach for large-scale production of graphene [7]. Moreover, the applications of reduced graphene oxide obtained via such chemical treatment in catalysis [2], sensors [8] and energy storage [9–11] have been widely studied. Various chemicals include hydrazine [6,12], borohydrides [13–17], ascorbic acid [18], KOH [8], sulphur-containing compounds [19], metal-acid [20], sugars [21], amino acids [22] and others were reported for the reduction of GO. However, some of these chemicals are poisonous, explosive or corrosive. Besides, the reduction usually takes place in a hot solution for a very long time, as shown in Table S1 (Supporting information). Therefore, it is necessary to chemically reduced GO rapidly with mild chemicals under mild experimental conditions.

Sodium borohydride is a mild and inexpensive reducing agent that have wide applications in chemistry both in the laboratory and on an industrial scale [23,24]. There are also many researches on reducing GO by $NaBH_4$ [13–17]. However, the reduction typically takes place above 80 °C for several hours and many oxygen-containing functional groups remain on the obtained rGO, since $NaBH_4$ hardly reduces carboxylic acids [24] and its hydrolysis is quite slow under ambient conditions [25]. Chen *et al.* studied introducing variable-valence metal (Mn, Co, Ni and Al) ion (VVMI) to $NaBH_4$-reducing GO suspension at 90 °C for 1 h, and found that the VVMI can assist the removal of −COOH [15]. Zhuo *et al.* prepared graphene by reducing GO with $NaBH_4$ and using $Cu(NO_3)_2$ as a catalysis at room temperature. But the reduction process still takes a long time, and the content of $Cu(NO_3)_2$ must be limited to ensure the stability of the GO suspension [16].

Herein, we developed a novel and ultrafast method to synthesis of rGO at room temperature. The process was characterized by the introduction of sodium molybdate and hydrochloride acid to assist the reduction of GO by $NaBH_4$. The obtained rGOs were characterized by X-ray diffraction (XRD), UV–vis absorption spectroscopy, Raman spectroscopy, X-ray photoelectron spectroscopy (XPS) and electrochemical tests.

Graphite oxide was synthesized by the modified Hummers method from natural graphite powder [26]. 100 mg as-prepared graphite oxide was dispersed in 100 mL water under ultrasonication for 30 min to make a homogeneous graphene oxide colloidal dispersion. After the pH of this dispersion was adjusted to 9∼10 by the addition of 1 mol/L NaOH solution, 1 mmol Na_2MoO_4 and 800 mg $NaBH_4$ was dispersed in 100 mL of the GO dispersion by stirring. Then 10 mL 2 mol/L HCl was added gradually under constant stirring until no more bubbles appear in the dispersion (∼ 2 min). Once HCl was added, the brown colored dispersion turned

* Corresponding author.
E-mail address: konggang@scut.edu.cn (G. Kong).

https://doi.org/10.1016/j.cclet.2020.03.045

black immediately, suggesting the reduction of GO. Finally, an appropriate amount of H_2O_2 was added in the dispersion to remove the molybdenum, then the dispersion was filtered and washed with deionized water. The final products were freeze-dried, denoted rGO-Mo-HCl. The same preparation in the absence sodium molybdate or HCl was implemented for comparison, and the as-prepared samples were denoted rGO-HCl and rGO-Mo, respectively. Besides, reduction samples with only $NaBH_4$ at 90 °C for 1 h which was denoted HrGO, is also used for comparison.

The morphology of rGO-Mo-HCl was observed by transmission electron microscope (TEM, Tecnai G2 F20, FEI, USA). The as-prepared GO and rGO samples were characterized by XRD (X'Pert^3 Powder, PANalytical, Netherlands) with Cu Kα radiation (λ = 0.15418 nm), Raman spectroscopy (LabRAM Aramis, HJY, France), UV–vis absorption spectroscopy (Cary 60, Agilent, USA), Fourier transform infrared spectroscopy (FTIR, VERTEX 70, Bruker, Germany) and XPS (Axis Ultra DLD, Kratos, UK).

To investigate the electrochemical performances of the rGO samples, cyclic voltammetry (CV), galvanostatic charge-discharge (GCD), and electrochemical impedance spectroscopy (EIS) experiments were performed using a CHI660E electrochemical workstation (CH Instrument, Chenhua Co., China) in a three-electrode cell. 1 mol/L Na_2SO_4 aqueous served as electrolyte. A platinum foil and a saturated calomel electrode served as the counter and reference electrodes, respectively. The working electrode was prepared by mixing 90 wt% rGO-Mo-HCl powder and 10 wt% polytetrafluoroethylene (PTFE) into slurry, followed by pressing on nickel foam (1×1 cm^2) and drying at 60 °C for 12 h. From the galvanostatic discharge curves, the specific capacitance (C) was estimated using the formula $C=(I \times \Delta t)/(m \times \Delta V)$, where I is the discharge current (A), Δt is the discharge time (s), m is the mass of the active materials in the electrode (g), and ΔV is the operating potential window (V) during the discharge [27].

Fig. 1a shows a TEM image of rGO-Mo-HCl. The graphene nanosheets are transparent and exhibit a curved and wrinkled appearance. The XRD patterns of GO, rGO-Mo, rGO-HCl, rGO-Mo-HCl and HrGO are shown in Fig. 1b. GO exhibits a (001) peak at $2\theta = 10.3^\circ$ with a large interlayer distance of 8.59 Å, due to the formation of oxygen-containing functional groups during chemical oxidation. After reduction with $NaBH_4$, Na_2MoO_4 and HCl, a broad (002) peak of rGO-Mo-HCl located at 23.9° appears and the (001) peak disappears, corresponding to the interlayer distance decreased to 3.72 Å. This implies that most of the oxygen-containing functional groups on GO were removed [14,15]. However, a broad peak near 10° of HrGO is still visible, implies the reduction of GO cannot be completed when $NaBH_4$ is used alone. Furthermore, the XRD patterns of rGO-Mo and rGO-HCl show a broad (001) peak near 10° which is similar with that of GO. It is probably because in the absence of HCl, the system is relatively stable and almost no reaction occurs; while in the absence of Na_2MoO_4, GO can hardly be reduced although the $NaBH_4$ is consumed. This also indicates a synergistic mechanism among Na_2MoO_4, $NaBH_4$ and HCl during reduction.

Fig. 1c shows the UV–vis absorption spectra of GO and rGOs. GO exhibits a maximum absorption peak at about 231 nm corresponding to π-π^* transition of aromatic C—C bonds and a shoulder at 298 nm corresponding to n-π^* transition of C=O bonds [18]. The peak patterns of rGO-Mo and rGO-HCl are almost similar with that of GO. However, the maximum absorption peak of rGO-Mo-HCl and HrGO redshifts to approximately 270 nm and the shoulder peak at 298 nm disappeared, suggesting the restoration of electronic conjugation within the graphene sheets [14].

Raman spectroscopy was employed to reflect the detailed structural information of GO and rGOs. In Fig. 1d, the Raman spectra of GO and rGOs display D band and G band at approximately 1352 and 1598 cm^{-1}, respectively. The G band relates to the bond stretching of sp^2 carbon pairs, whereas the D band relates to the breathing modes of sp^2 carbon rings that are activated by defects [16,28]. The intensity ratio of D and G bands (I_D/I_G) of rGO-Mo (0.95) and rGO-HCl (0.98) increases slightly compared to GO (0.94), which can be explained as the exfoliation by sonication making the size smaller. As for HrGO and rGO-Mo-HCl, the I_D/I_G shows obvious increase possibly due to the decrease in size of the in-plane sp^2 domains and increase in edge of the sheets when sp^2 domains are torn apart by the removal of oxygen-containing functional groups [6,16]. And the I_D/I_G of rGO-Mo-HCl (1.53) is higher than that for HrGO (1.21) indicating the deoxygenation is more efficient than the latter`s.

The chemical structure of GO and rGO samples were studied by FTIR and the data is present in Fig. S1 (Supporting information). The spectrum of GO illustrates the characteristic peaks including O—H stretching vibration peak of intercalated water at 3414 cm^{-1}, C=O stretching vibration peak in carboxyl and carbonyl at 1720 cm^{-1}, O—H deformation peak of carboxyl groups at 1405 cm^{-1}, C—OH and C—O—C stretching vibration peaks at 1229, 1124 and 1050 cm^{-1} [29,30]. The peak at 1620 cm^{-1} can be attributed to C=C skeletal vibrations of unoxidized graphitic domains or stretching deformation vibration of intercalated water [32]. These peaks are still visible in the spectra of rGO-Mo and rGO-HCl, but peaks for oxygen-containing functional groups are significantly decreased or disappeared in rGO-Mo-HCl and HrGO. In addition, the peaks at 1720 cm^{-1} and 1405 cm^{-1} are entirely disappeared in rGO-Mo-HCl, demonstrating the removal of carboxyl and carbonyl.

In order to obtain detailed information on the functional groups, we performed XPS on GO, and rGO samples. As shown in Fig. 2a, the XPS survey spectra of all samples exhibit the similar behavior, in which two peaks at 284.6 eV and 532.9 eV are corresponded to C 1s and O 1s, respectively. However, the intensity of O 1s peak in rGO samples is much weaker than that in GO indicating the removal of oxygen-containing functional groups after reduction. Fig. 2c displays the high resolution C 1s spectrum

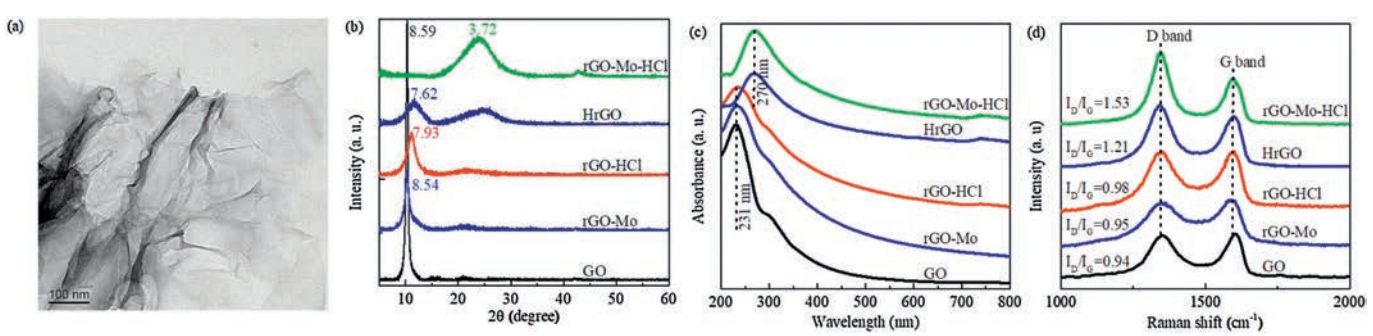

Fig. 1. (a) TEM image of rGO-Mo-HCl. (b) XRD patterns, (c) UV–vis and (d) Raman spectra of GO, rGO-Mo, rGO-HCl, HrGO and rGO-Mo-HCl.

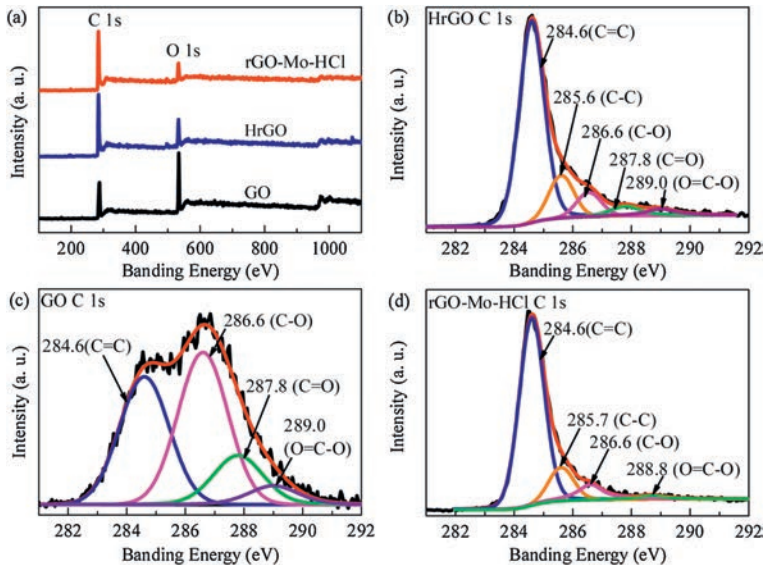

Fig. 2. (a) XPS survey spectra of GO, HrGO and rGO-Mo-HCl. C 1s spectra of (b) HrGO, (c) GO and (d) rGO-Mo-HCl.

of GO, which consists four components of the carbon bond, namely, C—C/C=C (284.6 eV), C—O (286.6 eV), C=O (287.8 eV) and O—C=O (289.0 eV) [6,14]. After reduction, the intensity of the peaks associated with the oxidized carbon decreased dramatically and a sp^3 carbon peak appears as shown in Figs. 2b and d. The relative percentage of each functional group assigned after the deconvolution C 1s spectra and C/O ratio are listed in Table S2 (Supporting information). It is obvious that the reduction process can lead an increase of C=C from 36.15% to approximately 70% and a significant decrease of oxygen-containing functional groups. Furthermore, for rGO-Mo-HCl, the C/O ratio increased to 6.5 and the relative atomic percentage of C=O/O—C=O is as low as 1.96%, whereas for HrGO, the C/O ratio is 4.6 and the relative atomic percentage of C=O and O—C=O are 3.54% and 3.93% respectively. This indicates that sodium borohydride, sodium molybdate and hydrochloric acid has more efficient reduction capacity in the reduction of GO than sodium borohydride alone, and sodium molybdate and hydrochloric can assist to reduce C=O and COOH. A probable reduction mechanism is discussed in detail in later paragraphs.

Scheme 1 illustrates the probable mechanism for the reduction of GO by sodium borohydride, sodium molybdate and hydrochloric

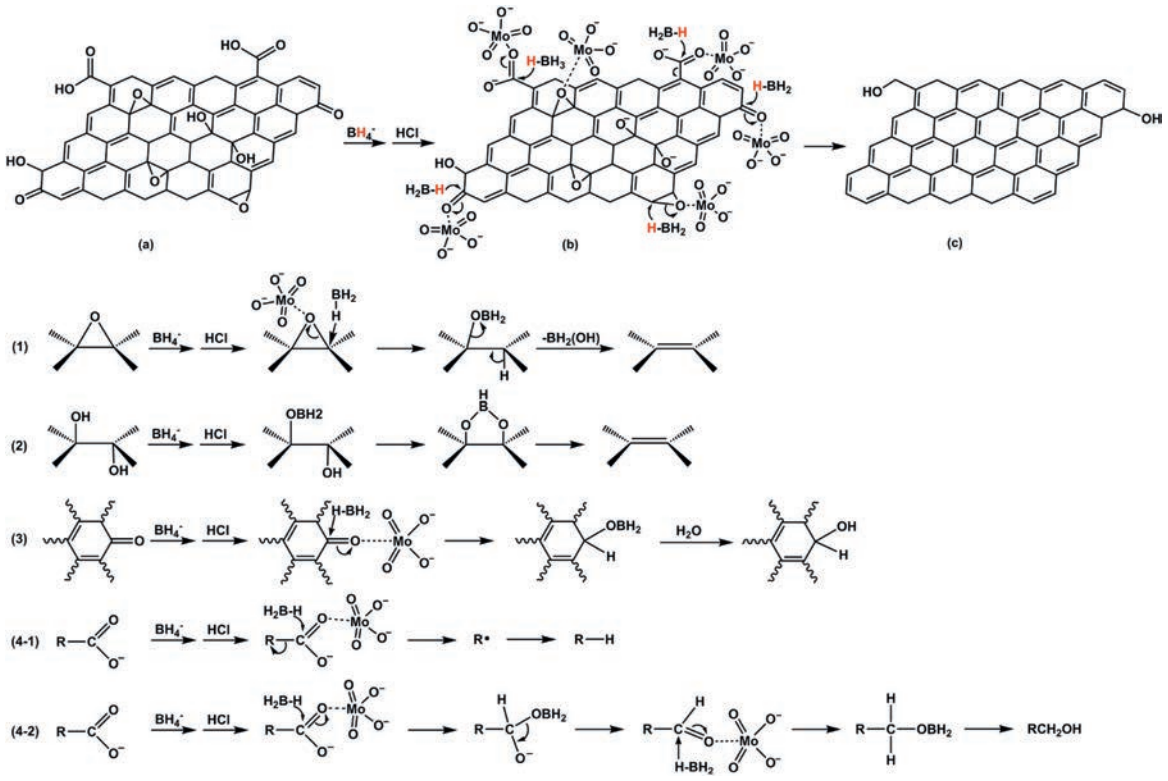

Scheme 1. A probable mechanism for the reduction of graphene oxide.

acid. At ordinary temperatures, sodium borohydride is quite stable in basic solution since the hydrolysis of borohydride produces the strongly basic metaborate ion, but reacts with hydrogen ions as the pH is lowered [31]. So that the added HCl will react rapidly with $NaBH_4$ and form the active reducing species, diborane (reaction 1) [25].

$$NaBH_4 + HCl \rightarrow H_2 + NaCl + (BH_3)_{aq}. \quad (1)$$

In addition, the central Mo(VI) of MoO_4^{2-} will coordinate with oxygen atoms of the oxygen-containing functional groups on GO due to its Lewis acid property. The coordination is considered to increase the positive charge on the carbon atom, so that the nucleophilic attack to carbon atom and the reduction of GO will be facilitated [32]. Scheme 1(1) shows the probable mechanism for de-epoxide of GO. The hydride anion in diborane as a nucleophile attacks the electrophilic carbon of the C—O and opens the epoxy group to form C—H and C—OBH_2, then the $BH_2(OH)$ is eliminated to form a double band. The probable mechanism for the reduction of hydroxyl (Scheme 1(2)) is due to the reaction of hydride anion in diborane and hydride cation in hydroxyl with release of H_2, resulting in the formation of an intermediate. The reaction may be followed by the elimination of $BH(OH)_2$, leading to recovery of C=C. As for carbonyl groups (Scheme 1(3)), it may be reduced to the corresponding alcohols. We speculate that there are two probable mechanisms for the reduction of carboxyl groups. One is decarboxylation (Scheme 1(4-1)), which is favorable because of the extended conjugation in carbon network [29,30,33]. The other is that carboxyl was reduced to the alcohols (Scheme 1(4-2)) [24,34].

Figs. 3a and b present the CV and GCD curves of the rGO-Mo-HCl electrode, respectively. The nearly rectangular shape of CV curves at various scan rates and approximately symmetric triangular shape of GCD curves indicating a good electrical double layer performance and low contact resistance [27]. As shown in Fig. 3c, the specific capacitances of rGO-Mo-HCl electrode at current densities of 1, 2, 3, 4 and 5 A/g are measured to be 139.8, 119.0, 111.7, 108.5 and 106.9 F/g, respectively. It is obvious that the specific capacitance decreases slightly with increasing current density. And the rGO-Mo-HCl electrode represents a significant improvement over GO electrode (Fig. S2 in Supporting information), and is better than the obtained with less reduced HrGO electrode (Fig. S3 in Supporting information), and is comparable to other reported chemically reduced graphene oxide [35,36]. The Nyquist plot obtained by the EIS tests in Fig. 3d exhibits a semicircle at high frequency and a near-vertical line at low frequency. Moreover, according to the Nyquist plot with an expanded view of the high frequency region (Fig. 3d inset), both the internal resistance and the charge transfer resistance are very low. These results demonstrate the good electrochemical performance of rGO-Mo-HCl and its high potential for electrode materials.

In summary, we have demonstrated an ultrafast and effective method to synthesize reduced graphene oxide at room temperature with Na_2MoO_4, $NaBH_4$ and HCl. Molybdate can coordinate with oxygen atoms of oxygen-containing groups on GO to increase the positive charge on carbon atom. And HCl can react with $NaBH_4$ and generate diborane in suit. Thus, the reduction of GO can complete within 2 min at room temperature. The product rGO-Mo-HCl has a higher C/O ratio and a lower content of carbonyl and carboxyl groups when compared with HrGO that reduced by $NaBH_4$ alone at high temperature. This high-efficient, energy-saving and low-cost method shows promising applications in large-scale production of rGO and graphene-based materials. And the rGO-Mo-HCl electrode exhibits good electrochemical performance with specific capacitance of 139.8 F/g allows it to be used for supercapacitors.

Declaration of competing interest

The authors declare that they have no known competing financial interests or personal relationships that could have appeared to influence the work reported in this paper.

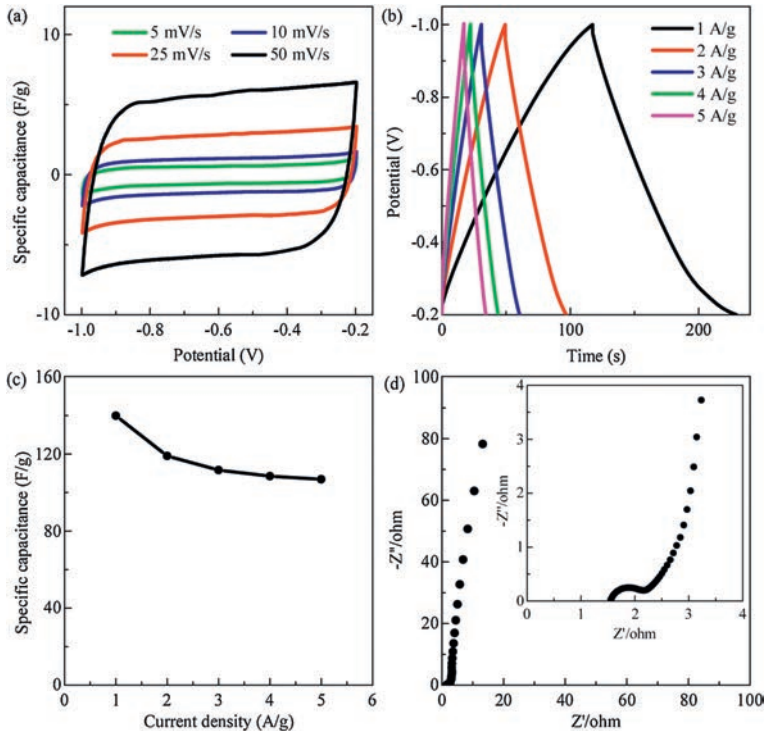

Fig. 3. Electrochemical results of rGO-Mo-HCl electrode: (a) CV curves; (b) GCD curves; (c) Specific capacitance at different current densities; (d) Nyquist plots. The inset in (d) shows an enlarged scale.

Appendix A. Supplementary data

Supplementary material related to this article can be found, in the online version, at doi:https://doi.org/10.1016/j.cclet.2020.03.045.

References

[1] K.S. Novoselov, V.I. Fal'Ko, L. Colombo, et al., Nature 490 (2012) 192–200.
[2] Y. Yang, M. Wu, X. Zhu, et al., Chin. Chem. Lett. 30 (2019) 2065–2088.
[3] X. Mu, X. Liu, K. Zhang, et al., Electron. Mater. Lett. 12 (2016) 296–300.
[4] W. Yang, G. Chen, Z. Shi, et al., Nat. Mater. 12 (2013) 792–797.
[5] J. Fu, X.H. Tan, Y.H. Li, X.J. Song, Chin. Chem. Lett. 27 (2016) 1541–1546.
[6] S. Stankovich, D.A. Dikin, R.D. Piner, et al., Carbon 45 (2007) 1558–1565.
[7] C.K. Chua, M. Pumera, Chem. Soc. Rev. 43 (2014) 291–312.
[8] Y. Tang, Q. Guo, Z. Chen, et al., Compos. Part A: Appl. Sci. Manufact. 116 (2019) 106–113.
[9] C. Peng, J. Yu, S. Chen, L. Wang, Chin. Chem. Lett. 30 (2019) 1137–1140.
[10] S. Zheng, L. Zheng, Z. Zhu, et al., Nano-Micro Lett. 10 (2018) 62.
[11] L. Lyu, K. dong Seong, J.M. Kim, et al., Nano-Micro Lett. 11 (2019) 88.
[12] O. Akhavan, R. Azimirad, H.T. Gholizadeh, F. Ghorbani, Int. J. Hydrogen Energy 40 (2015) 5553–5560.
[13] W. Gao, L.B. Alemany, L. Ci, P.M. Ajayan, Nat. Chem. 1 (2009) 403–408.
[14] H.J. Shin, K.K. Kim, A. Benayad, et al., Adv. Funct. Mater. 19 (2009) 1987–1992.
[15] C. Chen, T. Chen, H. Wang, et al., Nanotechnology 22 (2011) 405602.
[16] Q. Zhuo, J. Gao, M. Peng, et al., Carbon 52 (2013) 559–564.
[17] Z. Yang, Q. Zheng, H. Qiu, et al., New Carbon Mater. 30 (2015) 41–47.
[18] K.K.H. De Silva, H.H. Huang, M. Yoshimura, Appl. Surf. Sci. 447 (2018) 338–346.
[19] R. Yin, P. Shen, Z. Lu, J. Colloid Interf. Sci. 550 (2019) 110–116.
[20] S. Azizighannad, S. Mitra, Sci. Rep. 8 (2018) 10083.
[21] C. Xu, X. Shi, A. Ji, et al., PLoS One 10 (2015) e0144842.
[22] D.N.H. Tran, S. Kabiri, D. Losic, Carbon 76 (2014) 193–202.
[23] A. Abiko, S. Masamune, Tetrahedron Lett. 33 (1992) 5517–5518.
[24] M. Periasamy, M. Thirumalaikumar, J. Organometallic Chem. 609 (2000) 137–151.
[25] R.E. Davis, C.G. Swain, J. Am. Chem. Soc. 82 (1960) 5949–5950.
[26] N.I. Kovtyukhova, Chem. Mater. 11 (1999) 771–778.
[27] Y.Z. Liu, C.M. Chen, Y.F. Li, et al., J. Mater. Chem. A 2 (2014) 5730–5737.
[28] I.M. Leo, E. Soto, F. Vaquero, et al., Topics Catal. 60 (2017) 1183–1195.
[29] R.S. Dey, S. Hajra, R.K. Sahu, et al., Chem. Commun. 48 (2012) 1787–1789.
[30] H. Feng, R. Cheng, X. Zhao, et al., Nat. Commun. 4 (2013) 1539.
[31] H.I. Schlesinger, H.C. Brown, A.E. Finholt, et al., J. Am. Chem. Soc. 75 (1953) 215–219.
[32] S. Rayati, E. Bohloulbandi, S. Zakavi, Inorg. Chem. Commun. 54 (2015) 38–40.
[33] X. Gao, J. Jang, S. Nagase, J. Phys. Chem. C 114 (2010) 832–842.
[34] J.W. Simek, T. Tuck, K.C. Bush, J. Chem. Educ. 74 (1997) 107.
[35] M.D. Stoller, S. Park, Z. Yanwu, et al., Nano Lett. 8 (2008) 3498–3502.
[36] J. Chen, K. Sheng, P. Luo, et al., Adv. Mater. 24 (2012) 4569–4573.